SUPPORTING INFORMATION

Switching the Spin State of Diphenylcarbene via Halogen Bonding

Stefan Henkel,[†] Paolo Costa,[†] Linda Klute,[†] Pandian Sokkar,[‡] Miguel Fernandez-Oliva,[‡] Walter Thiel,[‡] Elsa Sanchez-Garcia,*[,‡] and Wolfram Sander*[,†]

[†]Lehrstuhl für Organische Chemie II, Ruhr-Universität Bochum, 44801 Bochum, Germany

[‡]Max-Planck-Institut für Kohlenforschung, 45470 Mülheim an der Ruhr, Germany

Contents

Spectroscopic Data

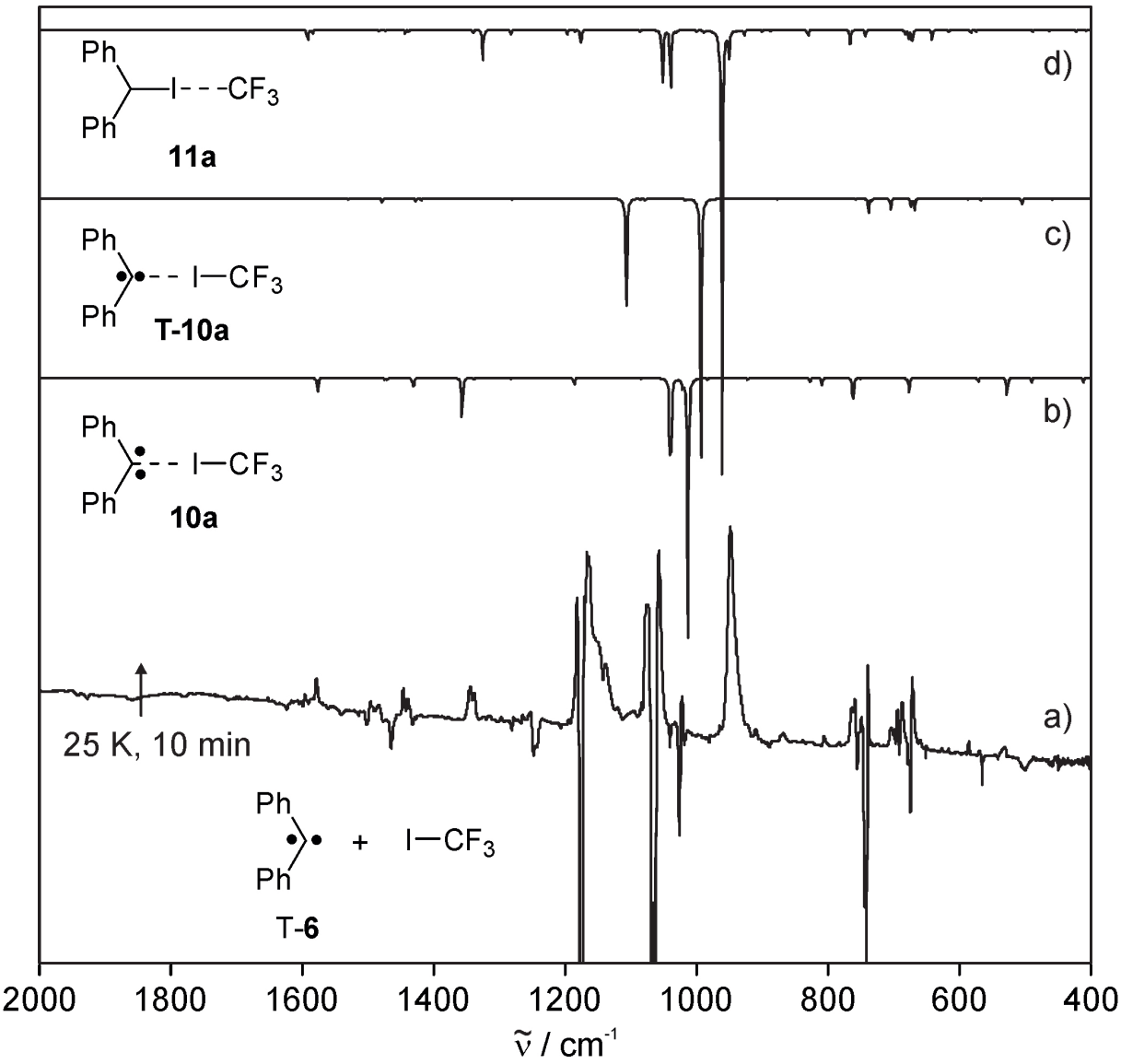

Figure S1. IR spectrum of the reaction of DPC **6** with ICF_3. a) IR difference spectrum obtained upon annealing of an argon matrix containing triplet carbene **6** and 1 % of ICF_3 to 25 K for 10 min. b) Calculated IR spectrum of singlet complex **10a** (B97-D3/def2-TZVP). c) Calculated IR spectrum of triplet complex T-**10a** (B97-D3/def2-TZVP). d) Calculated IR spectrum of the complex **11a** (B97-D3/def2-TZVP).

Table S1. Calculated and experimental IR frequencies of **S-10a**.				
Mode	$\tilde{\nu}$ / cm^{-1}			Assignment
	Exp. (I_{rel}) [a]	Calc. gas phase (I_{rel})[b]	Calc. QM/MM[d]	
20	504 (4)	489(2)	488	C-H def. (out-of-plane)
22	529 (3)	527(7)	540	C-C-C def. (out-of-plane) (carbene)
23	568 (2)	571(1)	570	Skel. Vibr.
27	679 ([c])	676(5)	684	C-H def. (out-of-plane)
28		677(1)	686	C-H def. (out-of-plane)
31	764 (11)	761(9)	765	C-H def. (out-of-plane)
33	838 (3)	827(2)	833	C-H def. (out-of-plane)
44	1078 (100)	1013(100)	1022	F_3C-I str.
47	1103 (58)	1038(25)	1070	C-F_3 asym. str.
48		1040(27)	1078	C-F_3 asym. str.
60	1338/1344 (64)	1357(16)	1355	C-C-C asym. str. (carbene)
61	1439 (3)	1430(3)	1418	C=C str. Ring
62		1432(2)	1421	C=C str. Ring
63	1496 (5)	1471(1)	1467	C=C str. Ring
64		1474(1)	1475	C=C str. Ring
67	1578 (20)	1576(6)	1570	C=C str. Ring
[a] Measured in argon at 3 K. Integrated intensities refer to the difference spectrum. [b] Calculated at the B97D3/def2-TZVP level of theory. [c] Intensity not assigned due to overlapping of the signal. [d] Calculated at the B97D3/dfe2-TZVP//CHARMM level of theory in an Ar matrix.				

Table S2. Calculated and experimental IR frequencies of **11a**.				
Mode	$\tilde{\nu}$ / cm^{-1}			Assignment
	Exp. (I_{rel}) [a]	Calc. gas phase (I_{rel})[b]	Calc. QM/MM[c]	
27	672(14)	671(3)	664	Skel. Vibr.
28	686(4)	677(2)	686	C-H def. (out-of-plane)
29	693(2)	682(1)	697	C-H def. (out-of-plane)
30	750(4)	743(2)	743	C-H def. (out-of-plane)
31	757(5)	766(4)	767	C-H def. (out-of-plane)
41	949(100)	961(100)	962	F_3C-I str.
47	1139(23)	1039(13)	1047	C-F_3 asym. str.
48	1149(20)	1051(14)	1056	C-F_3 asym. str.
62	1448(1)	1444(1)	1428	C=C str. Ring
67	1485(1)	1584(1)	1572	C=C str. Ring
68		1592(2)	1580	C=C str. Ring
[a] Measured in argon at 3 K. Integrated intensities refer to the difference spectrum. [b] Calculated at the B97D3/def2-TZVP level of theory, not a minimum. [c] Calculated at the B97D3/dfe2-TZVP//CHARMM level of theory in an Ar matrix.				

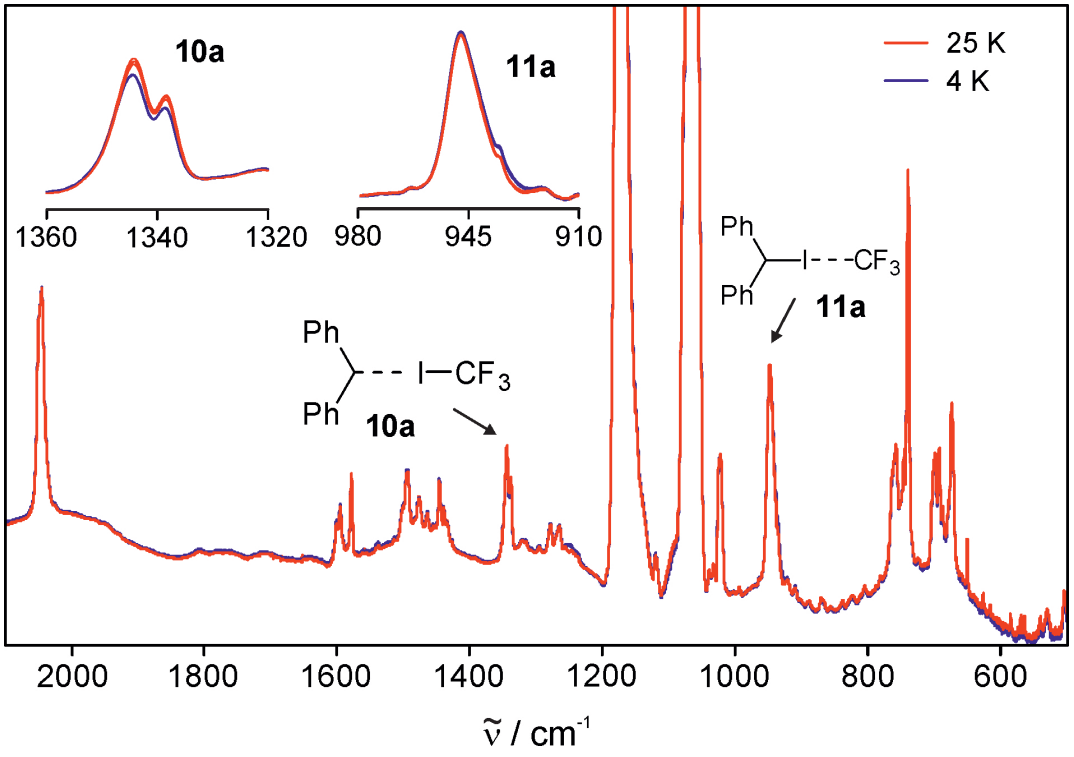

Figure S2. IR spectra showing the interconversion between complexes **10a** and **11a** upon cycling the temperature between 25 K (red spectra) and 4 K (blue spectra). Insets show the characteristic signals of **10a** and **11a**.

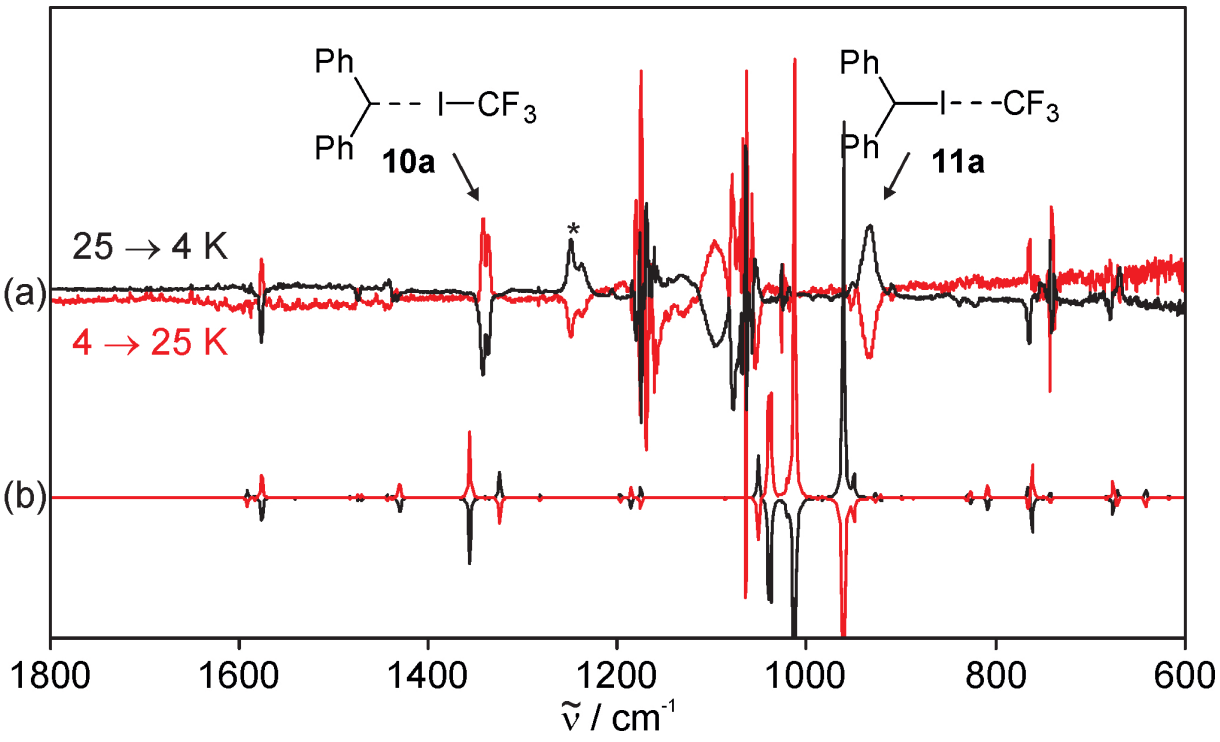

Figure S3. IR difference spectra showing the interconversion between complexes **10a** and **11a** upon cycling the temperature between 25 and 4 K. a) IR difference spectrum obtained on warming to 25 K (red) and on cooling back to 4 K (black). Bands of the CF_3 radical are labeled with an asterisk. b) Calculated IR difference spectra (B97-D3/def2-TZVP) of the conversion of **11a** to **10a** (red) and of **10a** to **11a** (black).

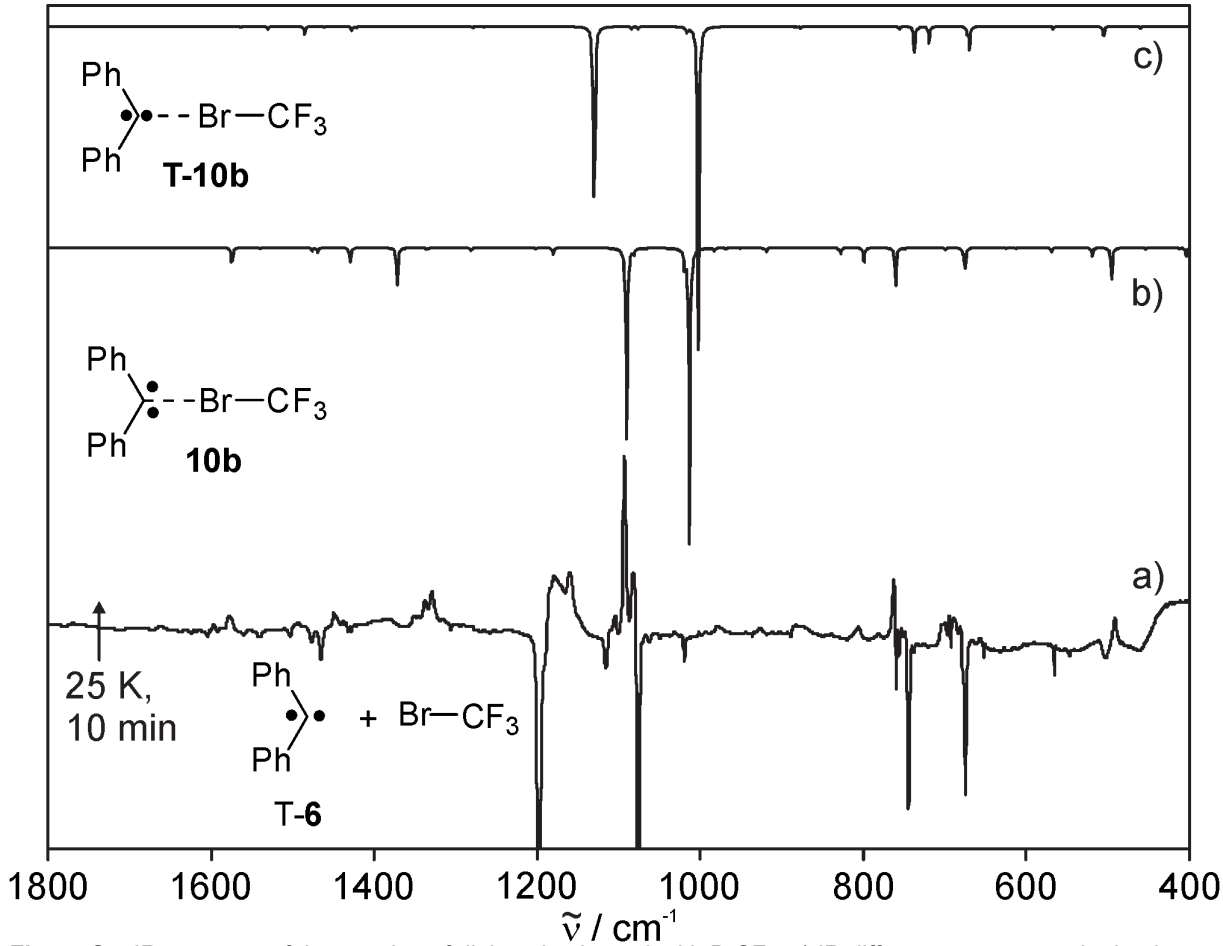

Figure S4. IR spectrum of the reaction of diphenylcarbene **6** with $BrCF_3$. a) IR difference spectrum obtained upon annealing of an argon matrix containing triplet carbene **6** and 0.5 % of $BrCF_3$ to 25 K for 10 min. b) Calculated IR spectrum of singlet complex **10b** (B97-D3/def2-TZVP). c) Calculated IR spectrum of triplet complex T-**10b** (B97-D3/def2-TZVP).

Table S3. Calculated and experimental IR frequencies of **S-10b**.

	$\tilde{\nu}$ / cm^{-1} **10b**		$\tilde{\nu}$ / cm^{-1} **10a**
#	Calc. (Int.)[a]	Exp. (Int.)[b,c]	Exp. (Int.)[a]
20	494 (13)	492 (8)	504 (4)
			529 (3)
23	568 (2)	565 (2)	568 (2)
27	674 (7)	675/680 (4)	679 ([d])
31	760 (13)	762 (18)	764 (11)
32	798 (5)	809 (2)	838 (3)
44	1013 (100)	1093 (71)	1078 (100)
49	1089 (34)	1161 (100)	1103 (58)
50	1090 (39)		
54	1181 (2)	1198 (2)	
60	1371 (15)	1329/1337 (28)	1338/1344 (64)
61	1429 (4)	1435 (3)	1439 (3)
62	1430 (2)		
63	1469 (2)	1496 (2)	1496 (5)
64	1476 (1)		
67	1574 (5)	1576 (9)	1578 (20)

[a] Calculated at the B97D3/def2-TZVP level of theory [b] Measured in argon at 3 K. [c] Integrated intensities refer to the difference spectrum. [d] Intensity not assigned due to overlapping of the signal.

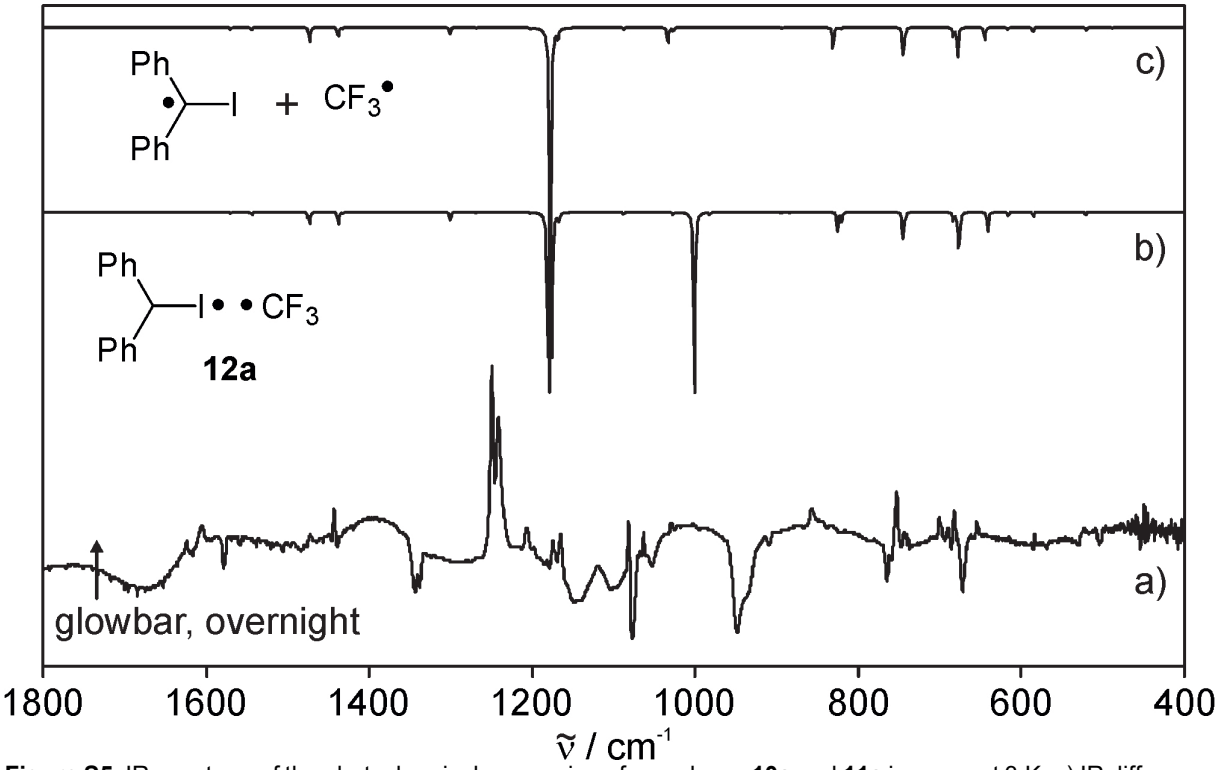

Figure S5. IR spectrum of the photochemical conversion of complexes **10a** and **11a** in argon at 3 K. a) IR difference spectrum obtained upon keeping a matrix containing complexes **10a** and **11a** inside an IR spectrometer overnight. b) Calculated IR spectrum of radical pair **12a** (B97-D3/def2-TZVP). c) Superposition of the calculated IR spectra of Ph_2CI and CF_3 radical (B97-D3/def2-TZVP).

Table S4. Calculated and experimental IR frequencies of **12a**.

Mode	$\tilde{\nu}$ / cm^{-1}			Assignment
	Exp. (I_{rel}) [a]	Calc. gas phase (I_{rel})[b]	Calc. QM/MM[c]	
22	522(1)	520(2)	528	C-H def. (out-of-plane)
23	583(1)	584(3)	579	Skel. Vibr.
24	614(1)	615(3)	611	Skel. Vibr.
26	654(4)	641(16)	629	Skel. Vibr.
27	682(7)	675(21)	662	F_3C-I str.
28	689(3)	677(20)	684	C-H def. (out-of-plane)
29	700(7)	683(6)	691	C-H def. (out-of-plane)
31	752(19)	745(18)	749	C-H def. (out-of-plane)
34	857(6)	824(13)	827	C-I str.
46	1082(12)	1027(2)	1013	C-H def. (in-plane)
47		1088(2)	1071	C-H def. (in-plane)
50	1206(6)	1167(5)	1117	C-C-C sym. str. (carbene)
52	1242(100)	1176(100)	1167	C-F_3 asym. str.
53	1249(90)	1181(90)	1170	C-F_3 asym. str.
62	1443(6)	1438(9)	1425	C=C str. Ring
63	1473(2)	1473(8)	1475	C=C str. Ring

[a] Measured in argon at 3 K. Integrated intensities refer to the difference spectrum. [b] Calculated at the B97D3/def2-TZVP level of theory. [c] Calculated at the B97D3/dfe2-TZVP//CHARMM level of theory in an Ar matrix.

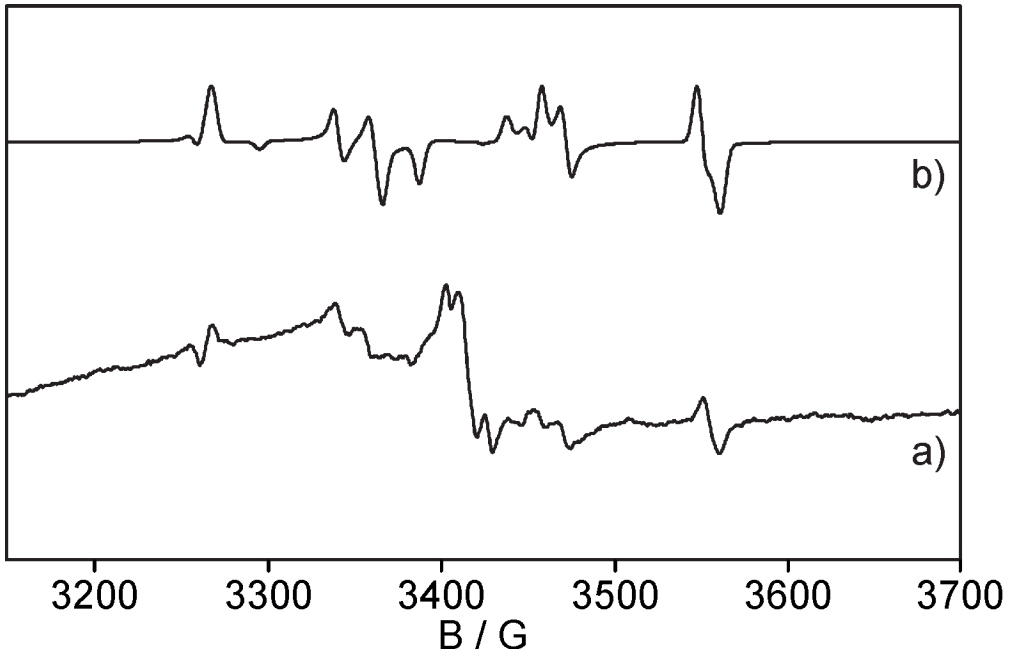

Figure S6. EPR spectrum of CF_3 radicals. a) EPR spectrum obtained upon irradiation (450 nm) of an annealed matrix containing diphenylcarbene **6** and 1 % of ICF_3. b) Simulated EPR spectrum (μ = 9.575 GHz, g1 = 2.0023 g2 = 1.994 g3 = 2.004 A1 = 823 MHz A2 = 235 MHz A3 = 270 MHz)

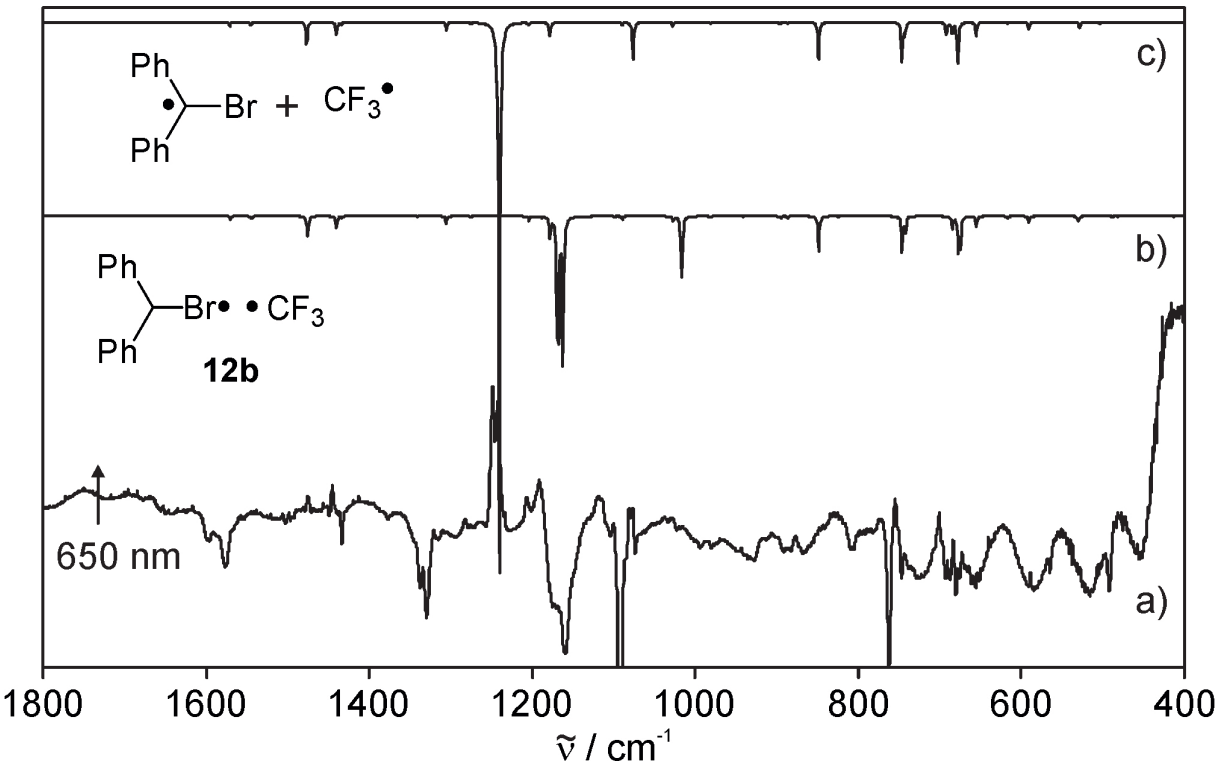

Figure S7. IR spectrum of the photochemical conversion of complexes **10b** in argon at 3 K. a) IR difference spectrum obtained upon irradiation of complex **10b** with 650 nm light. b) Calculated IR spectrum of radical pair **12b** (B97-D3/def2-TZVP). c) Superposition of the calculated IR spectra of Ph_2CBr and CF_3 radical (B97-D3/def2-TZVP).

Table S5. Calculated and experimental IR frequencies of **12b**. The calculated frequencies of CF_3 and Ph_2CBr radical at the same level are given for comparison.

Mode	$\tilde{\nu}$ / cm^{-1}			
	Exp. (I_{rel}) [a]	Calc. gas phase (I_{rel})[b]	Calc. CF_3 radical (I_{rel})	Calc. (I_{rel})[c]
22	528(2)	527(4)		528(1)
23	588(3)	592(5)		591(2)
24	611(1)	618(1)		617(0)
26	641(3)	659(7)		655(3)
27	683(11)	674(37)	678(1)	
28	689(6)	675(1)		678(8)
29	700(8)	681(10)		685(2)
31	754(23)	740(9)		743/746(9)
32		745(20)		
34	876(5)	855(20)		848(8)
44	1082(22)	1021(44)	1033(5)	
51	1243(100)	1166(100)	1178/1178(100)	
52	1249(88)	1170(98)		
62	1445(4)	1446(9)		1440(3)
63/64	1475(7)	1478/1479(16)		1477/1478(4)

[a] Measured in argon at 3 K. Integrated intensities refer to the difference spectrum. [b] Calculated at the B97D3/def2-TZVP level of theory. [c] Relative to the summed intensity of the most intense vibration of the CF_3 radical.

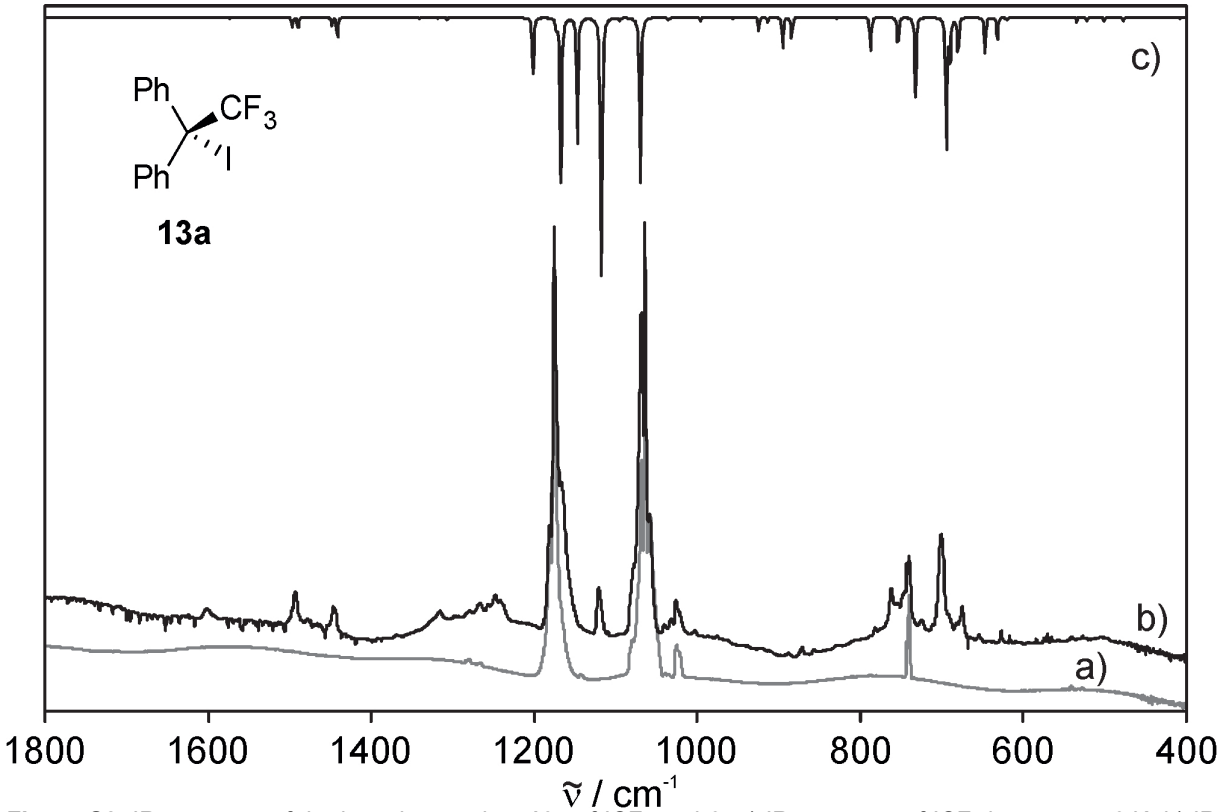

Figure S8. IR spectrum of the insertion product **13a** of ICF_3 and **6**. a) IR spectrum of ICF_3 in argon at 3 K. b) IR spectrum obtained after 450 nm irradiation of the annealed matrix. c) Calculated IR spectrum of **13a** (B97-D3/def2-TZVP).

Table S6. Experimental (Ar, 3 K) and calculated (B97-D3/def2-TZVP) frequencies of **13a**.

Mode	$\tilde{\nu}$ / cm^{-1}	
	Exp. (I_{rel}) [a]	Calc. gas phase (I_{rel}) [b]
25	654(5)	646(13)
26	674(15)	680(12)
27	700(100)	690(15)
28		694(41)
29	740(31)	732(25)
30	761(14)	754(9)
31	825(6)	787(11)
46	[c]	1070(61)
49	[c]	1117(100)
50	[c]	1147(42)
51	[c]	1167(56)
54	[c]	1201(17)
61	1446(12)	1441(7)
62		1448(3)
63	1493(13)	1490(4)
64		1497(4)

[a] Measured in argon at 3 K. Integrated intensities refer to the difference spectrum. [b] Calculated at the B97D3/def2-TZVP level of theory. [c] Signal not assignable due to overlap with the signals of ICF_3.

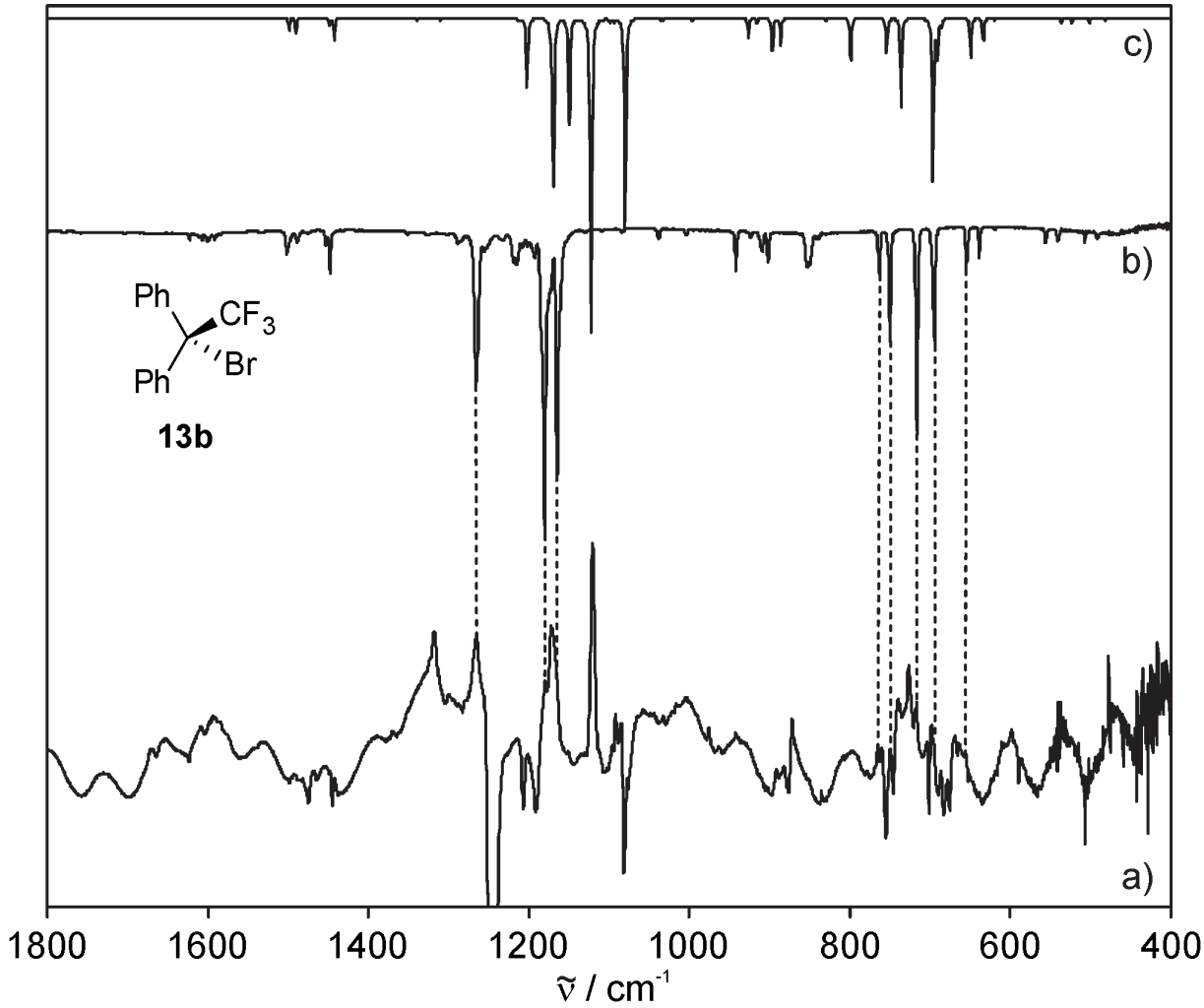

Figure S9. IR spectrum of the insertion product **13b** of $BrCF_3$ and **6**. a) IR difference obtained on annealing of an argon matrix containing **12b**. b) IR spectrum of **13b** in argon at 10 K. (Trifluoromethyl)diphenylmethyl bromide **13b** was prepared according to literature procedure: Ohwada, T.; Shudo, K. *J. Am. Chem. Soc.* **1988**, *110*, 1862. c) Calculated IR spectrum of **13b** (B97-D3/def2-TZVP).

Table S7. Experimental (Ar, 10 K) and calculated (B97-D3/def2-TZVP) frequencies of **13b**.		
Mode	$\tilde{\nu}$ / cm^{-1}	
	Exp. (I_{rel}) [a]	Calc. gas phase (I_{rel})[b]
18	491 (1)	482 (1)
19	507 (1)	501 (1)
20	540 (2)	523 (1)
21	556 (2)	536 (1)
22	619 (0.3)	619 (0.5)
24	639 (4)	633 (7)
25	655 (7)	649 (11)
27	694 (24)	691 (12)
28	717 (35)	696 (43)
29	749 (18)	736 (24)
30	763 (7)	754 (9)
31	853 (15)	798 (13)
34	902 (5)	886 (7)
35	909 (5)	897 (11)
36	924 (1)	915 (2)
37	942 (5)	926 (5)
42	1005 (1)	996 (1)
43		997 (1)
44	1038 (2)	1032 (1)
45		1036 (1)
46	1165 (62)	1080 (61)
49	1181 (100)	1122 (100)
50	1215 (14)	1150 (32)
51	1233 (5)	1169 (46)
54	1266 (50)	1201 (3)
55		1202 (20)
57	1289 (2)	1310 (1)
58	1302 (0.4)	1320 (0.4)
59	1327 (1)	1339 (1)
60	1352 (0.5)	1355 (0.2)
61	1449 (6)	1443 (6)
62	1453 (2)	1448 (2)
63	1489 (3)	1490 (4)
64	1503 (6)	1499 (3)
71	3046 (3)	3120 (5)
72		3120 (5)
73	3075 (8)	3130 (13)
74		3132 (11)
75	3098 (1)	3138 (4)
76	3109 (1)	3147 (3)
78	3171 (0.2)	3182 (1)
[a] Measured in argon at 10 K. [b] Calculated at the B97D3/def2-TZVP level of theory.		

Computational Results

Table S8. Stabilization energies and relative energies of the complexes between **6** and methanol, and the type-I complexes between diphenylcarbene **6** and CF_3I (**10a**) and between **6** and CF_3Br (**10b**). All energies in kcal/mol.			
Complexes	B97-D3/def2-TZVP		
	ΔEs	$\Delta Es_{c(BSSE)}$	Er (to the triplet state)
S-6…$HOCH_3$	-11.6	-10.8	1.2
T-6…$HOCH_3$	-6.1	-5.9	0.0
S-10a	-16.1	-15.8	-3.7
T-10a	-6.1	-6.0	0.0
S-10b	-11.0	-10.7	-0.5
T-10b	-4.2	-4.1	0.0

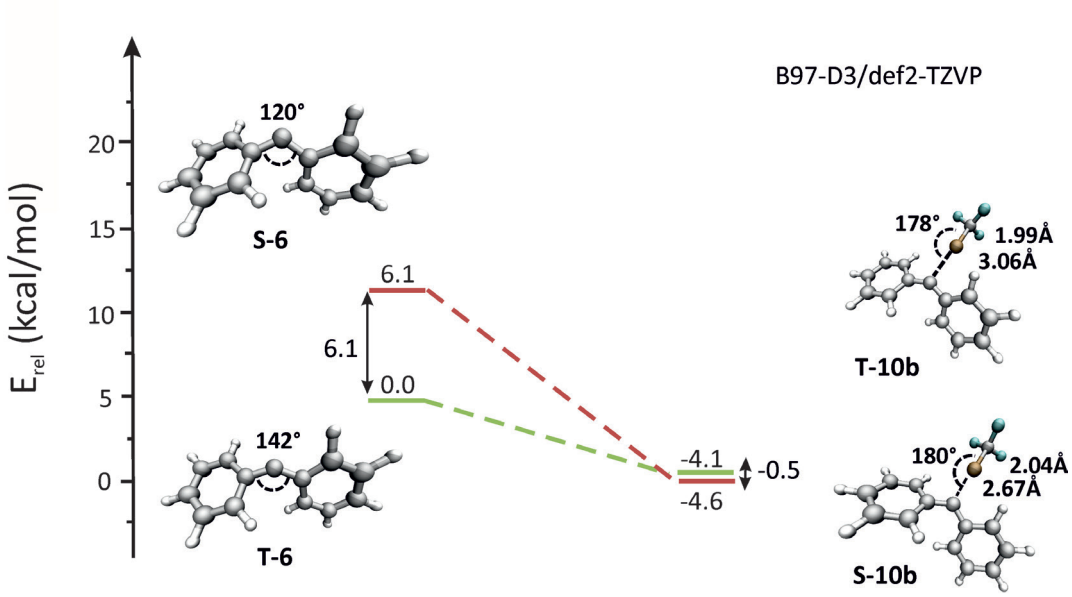

Fig. S10 Relative energies (including BSSE correction) and relevant geometric parameters of singlet and triplet DPC and the corresponding halogen bonded complexes with CF_3Br in the gas phase computed at the B97-D3/def2-TZVP level of theory.

Natural Bond Orbital (NBO) analysis

The main NBO interactions involved in both the H-bonded and the type-I X-bonded complexes of S-**6** are shown in Table S9. In both cases the main interaction is established between the lone pair of the carbene center (LP(C:)) and the anti-bonding orbital of the other molecule, BD*(I-C) for CF_3I and BD*(H-O) for the methanol complex. For the X-bonded complex an additional, weaker interaction can be identified, involving a back-donation from the lone pair of the iodine atom (LP3(I)) towards the empty p orbital on the carbene center (LP*(C:)). This interaction cannot be found in the H-bonded complex, since the H atom lacks the lone pair to engage in this back-donation.

Table S9. Main orbital interactions (NBO) between S-**6** and CF_3I (type-I complex) and between S-**6** and CH_3OH.				
Complex	Orbital interactions			
	Donor(i)-Acceptor(j)	E (kcal/mol)	E(j)-E(i) (a. u.)	F(i,j) (a. u.)
S-10a	LP(C:)-BD*(I-C)	53.69	0.21	0.096
	LP3(I)-LP*(C:)	5.60	0.10	0.024
S-6…$HOCH_3$	LP(C:)-BD*(H-O)	57.28	0.34	0.133

The main NBO interactions for complexes S-**10a** and **11a** are shown in Table S10. In complex **11a**, the main directional interaction is established between the lone pair at the carbon atom of CF_3 and the anti-bonding orbital on the C-I bond (LP1(CF_3)-BD*(C-I)) and it is diminished in comparison with the interaction in complex S-**10a**. This is related to the loss of linearity of the halogen bond, which allows a back-donation interaction from the lone pair of the iodine atom towards the same lone pair orbital on CF_3. This interaction helps to compensate the weaker primary interaction (with respect to the type-I complex), explaining the near degeneracy of both types of complexes.

Table S10. Main orbital interactions (NBO) between S-**6** and CF_3I type-I (**S-10a**) and type-II complexes (**11a**)

Complex	Orbital interactions			
	Donor(i)-Acceptor(j)	E (kcal/mol)	E(j)-E(i) (a. u.)	F(i,j) (a. u.)
S-10a	LP(C:)-BD*(I-C)	53.69	0.21	0.096
	LP3(I)-LP*(C:)	5.60	0.10	0.024
11a	LP1(CF_3)-BD*(C-I)	35.53	0.19	0.083
	LP3(I)-LP1(CF_3)	25.21	0.11	0.063

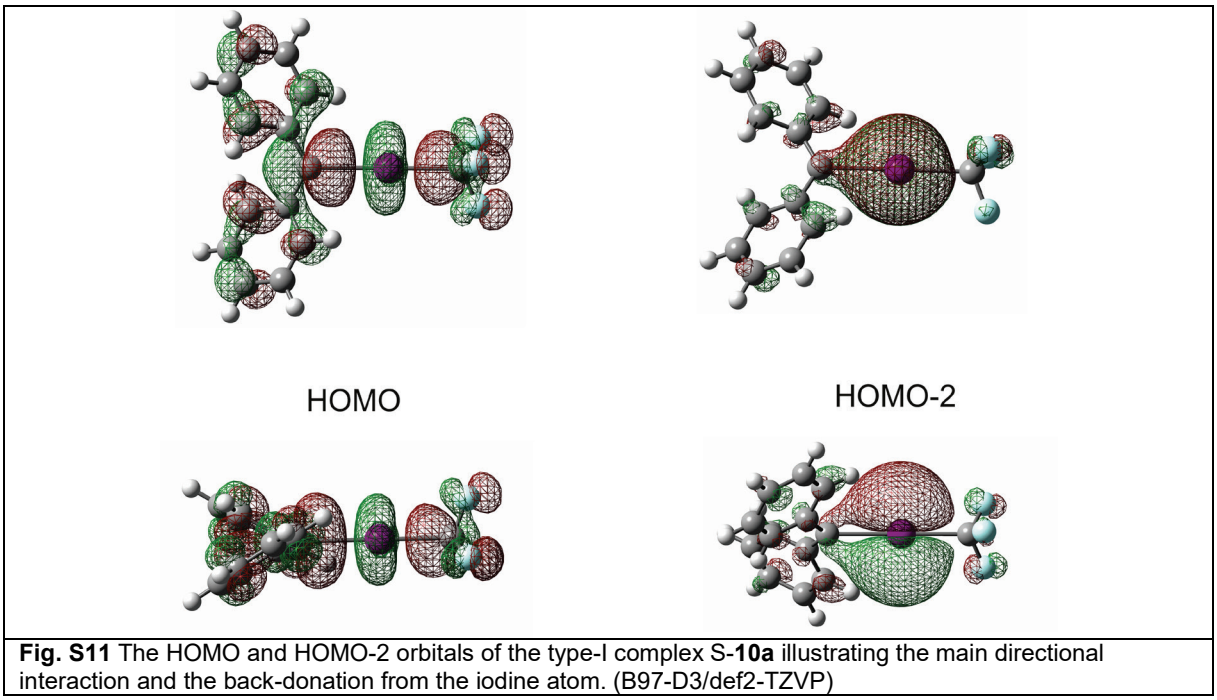

Fig. S11 The HOMO and HOMO-2 orbitals of the type-I complex S-**10a** illustrating the main directional interaction and the back-donation from the iodine atom. (B97-D3/def2-TZVP)

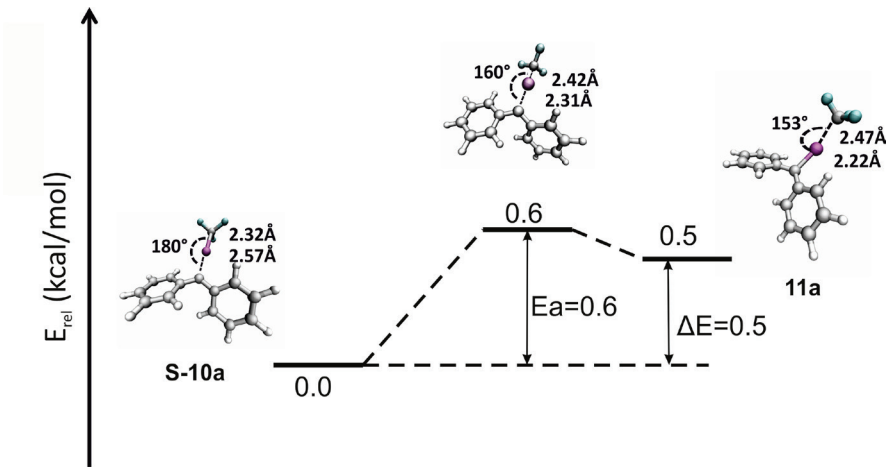

Fig. S12 Reaction path for the interconversion of the singlet complexes S-**10a** and **11a** (B97-D3/def2-TZVP).

CASSCF calculations

Active space:

From a general perspective, it would be desirable to define an active space that includes the π and π* orbitals from the two phenyl rings, the pi and sigma orbitals at the carbene center, and the C-I bonding and anti-bonding orbitals (without considering the lone pairs on the halogen atoms). The resulting active space with 16 electrons in 16 orbitals is too large to be practical. To limit the computational cost, we decided to include only 8 electrons and 8 orbitals in the active space. This selection was performed iteratively as follows.

The active space (8 electrons and 8 orbitals) was chosen differently for the singlet and triplet systems. The initial selection of orbitals was based on chemical intuition. The active space orbitals are shown in Figure S13. The carbene center has two nonbonded orbitals, σ_C and π_C. In addition to these two orbitals, the π and π* orbitals from the phenyl substituent were included. In general, halogen bonds are formed by the overlap of a σ-hole (in this case σ_I*) with electron-rich centers. Hence, the σ_I* and σ_I orbitals were also considered for the active space. For S-**10a**, among the variations tested, the fully occupied σ_C and unoccupied π_C configuration gives rise to low energy states (see below). Hence, we used this configuration. The σ_I* and σ_I orbitals were included as they are important for X-bond formation. In the case of T-**10a**, the σ_C and π_C orbitals are singly occupied and therefore included in the active space. The singly occupied π_C might favorably interact with the π-system of phenyl rings. Test calculations indicated that the inclusion of σ_I* and σ_I orbitals is not crucial for T-**10a** and therefore they are not part of the active space.

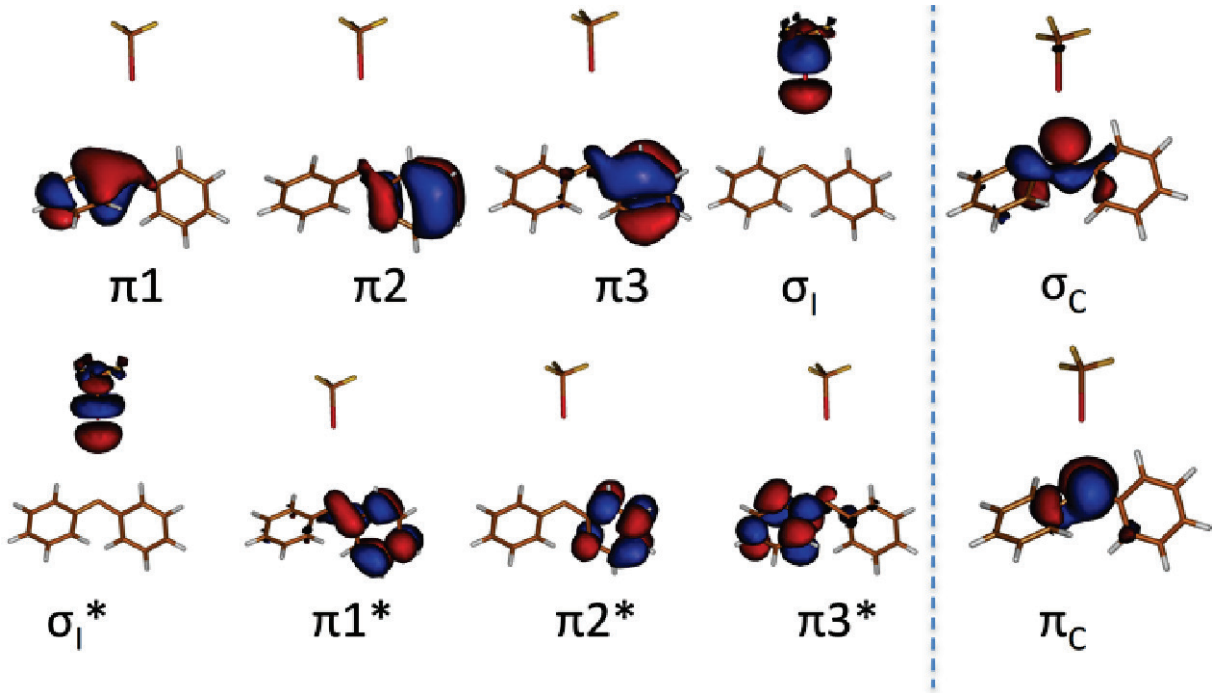

Fig. S13 Active space (8 electrons and 8 orbitals) used in the CASSCF MP2 calculations of the DPC-CF_3I complexes. Bonding and anti-bonding orbitals of the C-I bond in CF_3I are denoted as σ_I and σ_I*, respectively. The σ and π orbitals at the carbene center are denoted as σ_C and π_C, respectively. For the S-**10a** calculations, the σ_C and π_C orbitals were not included in the active space. For the T-**10a** calculations, σ_I and σ_I* were not included in the active space.

Multistate CASSCF calculations

We performed state-averaged multistate CASSCF (MS-CASSCF) calculations involving two states to calculate the vertical excitation energies for complex **10a** and **11a**. Single point MS-CASSCF calculations were performed for DFT geometries of **10a** and **11a** using an active space of 12 electrons and 12 orbitals. The active space included the ten orbitals shown in Fig. S13, in addition one π and one π^* orbital were also included (not shown). In the case of **10a**, the $\sigma_C^2\pi_C^0$ -> $\sigma_C^1\pi_C^1$ transition (at 944 nm) was dominant with the $\sigma_C^2\pi_C^0$ configuration having highest CI coefficient at S_0 state and $\sigma_C^1\pi_C^1$ at S_1 state. In the case of **11a**, the S_0 and S_1 states were found to have almost equal populations of $\sigma_C^2\pi_C^0$ and $\sigma_C^1\pi_C^1$. These transitions ($\sigma_C^2\pi_C^0$ -> $\sigma_C^1\pi_C^1$ and $\sigma_C^1\pi_C^1$ -> $\sigma_C^2\pi_C^0$) occur at 784 nm.

CASMP2 results with σ_C and π_C orbitals

As mentioned above, we did not include the σ_C and π_C orbitals (centered on carbene) in our ground state CASMP2 calculations of S-**10a**. Nevertheless, we ran a separate set of calculations with these two orbitals in the active space to compare the results. This way, the active space for these calculations consisted of the σ_C, π_C, π_1, π_1^*, π_2, π_2^*, σ_I and σ_I^* orbitals shown in Figure S13. The resulting potential energy scan (as a function of the C-I distance) at the CASMP2//DFT level is shown in Figure S14A. The comparison to the results shown in Figure 7A indicates that the inclusion of σ_C and π_C orbitals raises the energy of S-**10a** by 2.5 kcal/mol. In addition, with the inclusion of σ_C and π_C orbitals, the minimum in the PES corresponding to **11a** cannot be observed, not even in the 2D-scan (Figure 7B and Figure S14B).

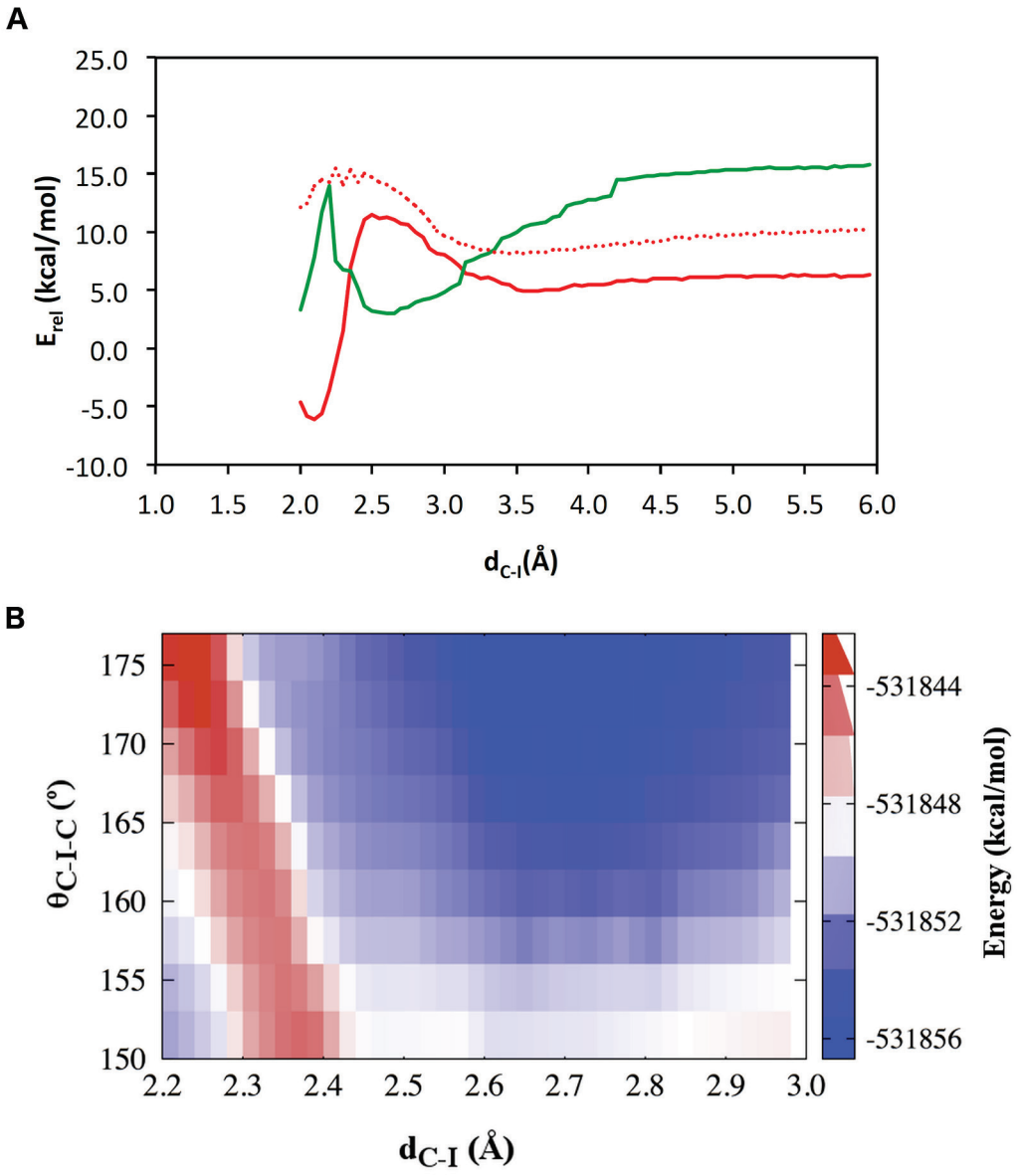

Fig. S14 A) Crossing point between singlet and triplet potential energy surfaces of **10a**. The potential energy profiles were obtained by performing constrained optimizations along the C-I distance. Potential energies are relative to that of S-**10a** (as shown in Figure 7B). B) 2D-potential energy scan, using the halogen bonding distance and angle as reaction coordinates, is shown as color-coded heat map. Potential energy surfaces were constructed by single point CASMP2 calculations on the DFT-optimized geometries. A different active space that includes σ_C and π_C orbitals was used for these calculations (see text).

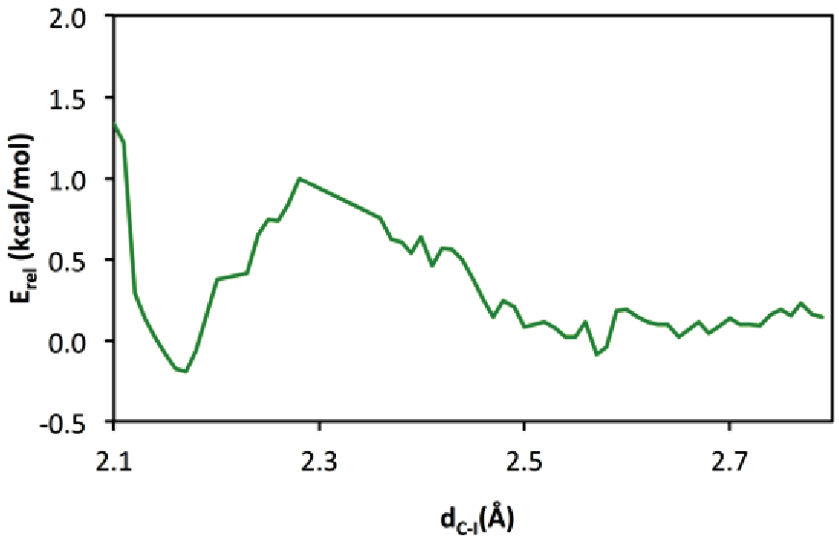

Fig. S15 The potential energy profile obtained by performing constrained optimizations along the C-I distance (2.1 - 2.8 Å, window of 0.01 Å) provides an estimate of the energy difference between S-**10a** and **11a**.

Cartesian coordinates of optimized structures

Table S11. Cartesian coordinates of **S-6** calculated at the B97D3/def2-TZVP level of theory.			
Atomic Symbol	x	y	z
C	-0.774	2.681	-1.245
C	-0.721	1.430	-0.641
C	0.000	1.233	0.577
C	0.678	2.358	1.133
C	0.690	3.580	0.476
C	-0.053	3.753	-0.704
H	-1.358	2.824	-2.152
H	-1.263	0.589	-1.067
H	1.201	2.223	2.077
H	1.242	4.419	0.895
H	-0.080	4.727	-1.190
C	0.000	0.000	1.288
C	0.000	-1.233	0.577
C	-0.678	-2.358	1.133
C	0.721	-1.430	-0.641
C	-0.690	-3.580	0.476
H	-1.201	-2.223	2.077
C	0.774	-2.681	-1.245
H	1.263	-0.589	-1.067
C	0.053	-3.753	-0.704
H	-1.242	-4.419	0.895
H	1.358	-2.824	-2.152
H	0.080	-4.727	-1.190
E=-501.0906205, ZPE=0.1797624			

Table S12. Cartesian coordinates of **T-6** calculated at the B97D3/def2-TZVP level of theory.			
Atomic Symbol	x	y	z
C	-0.570	2.985	-1.295
C	-0.561	1.668	-0.859
C	0.000	1.322	0.412
C	0.527	2.380	1.212
C	0.503	3.693	0.761
C	-0.041	4.008	-0.494
H	-0.999	3.226	-2.267
H	-0.984	0.878	-1.475
H	0.951	2.138	2.184
H	0.914	4.483	1.386
H	-0.055	5.038	-0.841
C	0.000	0.000	0.864
C	0.000	-1.322	0.412
C	-0.527	-2.380	1.212
C	0.561	-1.668	-0.859
C	-0.503	-3.693	0.761
H	-0.951	-2.138	2.184
C	0.570	-2.985	-1.295
H	0.984	-0.878	-1.475
C	0.041	-4.008	-0.494
H	-0.914	-4.483	1.386
H	0.999	-3.226	-2.267
H	0.055	-5.038	-0.841
E=-501.0996903, ZPE=0.1790838			

Table S13. Cartesian coordinates of **S-10a** calculated at the B97D3/def2-TZVP level of theory.			
Atomic Symbol	x	y	z
C	-3.690	-2.649	-0.804
C	-3.078	-1.404	-0.716
C	-1.844	-1.244	-0.017
C	-1.271	-2.395	0.596
C	-1.922	-3.620	0.553
C	-3.124	-3.755	-0.157
H	-4.614	-2.762	-1.368
H	-3.509	-0.544	-1.222
H	-0.325	-2.286	1.120
H	-1.486	-4.483	1.051
H	-3.613	-4.725	-0.215
C	-1.148	0.000	0.004
C	-1.842	1.246	0.020
C	-1.264	2.395	-0.591
C	-3.080	1.408	0.712
C	-1.914	3.621	-0.552
H	-0.316	2.286	-1.110
C	-3.691	2.653	0.796
H	-3.515	0.548	1.215
C	-3.120	3.758	0.152
H	-1.474	4.484	-1.048
H	-4.617	2.768	1.355
H	-3.608	4.729	0.207
C	3.749	-0.001	-0.003
I	1.426	-0.002	0.003
F	4.261	-1.179	-0.455
F	4.251	0.983	-0.801
F	4.257	0.200	1.245
E=-1136.9506684, ZPE=0.1942014			

Table S14. Cartesian coordinates of **T-10a** calculated at the B97D3/def2-TZVP level of theory.			
Atomic Symbol	x	y	z
C	-3.112	3.197	0.944
C	-2.809	1.847	0.832
C	-1.819	1.397	-0.096
C	-1.145	2.379	-0.878
C	-1.454	3.726	-0.746
C	-2.438	4.146	0.161
H	-3.872	3.519	1.653
H	-3.320	1.111	1.448
H	-0.383	2.055	-1.583
H	-0.929	4.459	-1.354
H	-2.675	5.203	0.260
C	-1.524	0.028	-0.202
C	-2.173	-1.209	-0.125
C	-1.497	-2.425	0.188
C	-3.578	-1.282	-0.398
C	-2.188	-3.629	0.238
H	-0.430	-2.397	0.390
C	-4.251	-2.494	-0.337
H	-4.108	-0.369	-0.657
C	-3.565	-3.676	-0.020
H	-1.650	-4.543	0.481
H	-5.319	-2.524	-0.543
H	-4.098	-4.623	0.022
C	3.734	-0.270	0.064
I	1.513	-0.073	0.001
F	4.107	-1.517	-0.277
F	4.194	-0.013	1.301
F	4.308	0.595	-0.791
E=-1136.9432396, ZPE=0.1929117			

Table S15. Cartesian coordinates of **11a** calculated at the B97D3/def2-TZVP level of theory.			
Atomic Symbol	x	y	z
C	3.164	-2.541	1.312
C	2.527	-1.339	1.028
C	1.638	-1.232	-0.066
C	1.409	-2.380	-0.857
C	2.062	-3.574	-0.584
C	2.938	-3.659	0.504
H	3.832	-2.614	2.167
H	2.688	-0.472	1.662
H	0.723	-2.306	-1.695
H	1.888	-4.444	-1.211
H	3.439	-4.598	0.725
C	0.967	0.017	-0.392
C	1.592	1.278	-0.101
C	0.894	2.445	0.304
C	2.986	1.411	-0.361
C	1.544	3.664	0.420
H	-0.156	2.365	0.567
C	3.619	2.644	-0.271
H	3.545	0.542	-0.694
C	2.907	3.778	0.126
H	0.986	4.535	0.753
H	4.678	2.718	-0.504
H	3.410	4.737	0.216
C	-3.512	-0.001	0.448
I	-1.249	-0.076	-0.531
F	-3.752	-1.038	1.291
F	-3.717	1.146	1.148
F	-4.450	-0.050	-0.538
E=-1137.0026935, ZPE=0.194331			

Table S16. Cartesian coordinates of **12a** calculated at the B97D3/def2-TZVP level of theory.			
Atomic Symbol	x	y	z
C	-2.989	3.193	0.733
C	-2.619	1.854	0.674
C	-1.414	1.449	0.032
C	-0.602	2.471	-0.524
C	-0.983	3.807	-0.464
C	-2.178	4.181	0.161
H	-3.910	3.470	1.242
H	-3.245	1.102	1.146
H	0.326	2.200	-1.019
H	-0.343	4.564	-0.913
H	-2.469	5.228	0.211
C	-1.069	0.047	-0.003
C	-2.017	-1.046	-0.020
C	-1.762	-2.311	0.567
C	-3.269	-0.872	-0.673
C	-2.708	-3.329	0.525
H	-0.815	-2.479	1.073
C	-4.208	-1.897	-0.714
H	-3.481	0.073	-1.165
C	-3.938	-3.133	-0.113
H	-2.487	-4.284	0.998
H	-5.151	-1.737	-1.233
H	-4.673	-3.934	-0.150
C	4.244	-0.205	0.037
I	1.018	-0.467	-0.050
F	4.739	-1.241	-0.641
F	4.630	-0.232	1.310
F	4.562	0.949	-0.542
E=-1136.9450171, ZPE=0.1936091			

Table S17. Cartesian coordinates of **13a** calculated at the B97D3/def2-TZVP level of theory.			
Atomic Symbol	x	y	z
C	-2.553	1.956	-1.640
C	-1.416	1.246	-1.278
C	-1.268	0.721	0.018
C	-2.301	0.929	0.941
C	-3.442	1.648	0.576
C	-3.576	2.162	-0.710
H	-2.644	2.346	-2.650
H	-0.628	1.083	-2.008
H	-2.233	0.547	1.950
H	-4.228	1.801	1.311
H	-4.468	2.717	-0.990
C	0.016	-0.024	0.326
C	1.266	0.759	-0.069
C	2.461	0.149	-0.467
C	1.242	2.156	0.068
C	3.595	0.911	-0.738
H	2.501	-0.930	-0.579
C	2.379	2.918	-0.198
H	0.332	2.650	0.390
C	3.559	2.299	-0.607
H	4.508	0.415	-1.056
H	2.336	3.998	-0.086
H	4.443	2.893	-0.824
C	0.171	-0.487	1.801
I	-0.130	-1.981	-0.855
F	0.198	0.599	2.622
F	-0.833	-1.284	2.232
F	1.324	-1.157	2.004
E=-1137.0415105, ZPE=0.1982742			

Table S18. Cartesian coordinates of **S-10b** calculated at the B97D3/def2-TZVP level of theory.			
Atomic Symbol	x	y	z
C	3.505	2.658	-0.800
C	2.905	1.409	-0.720
C	1.671	1.238	-0.027
C	1.084	2.381	0.584
C	1.730	3.607	0.560
C	2.933	3.753	-0.144
H	4.428	2.783	-1.361
H	3.344	0.555	-1.227
H	0.129	2.260	1.085
H	1.287	4.465	1.059
H	3.415	4.726	-0.195
C	0.977	0.000	0.005
C	1.668	-1.240	0.031
C	1.074	-2.381	-0.576
C	2.905	-1.415	0.716
C	1.717	-3.609	-0.558
H	0.115	-2.257	-1.071
C	3.503	-2.665	0.791
H	3.350	-0.562	1.220
C	2.924	-3.759	0.138
H	1.267	-4.465	-1.054
H	4.429	-2.793	1.346
H	3.403	-4.733	0.185
C	-3.747	0.002	-0.002
F	-4.232	1.187	-0.429
F	-4.227	-0.960	-0.819
F	-4.235	-0.224	1.235
Br	-1.715	0.003	0.004
E=-3414.1950902, ZPE=0.1946065			

Table S19. Cartesian coordinates of **T-10b** calculated at the B97D3/def2-TZVP level of theory.			
Atomic Symbol	x	y	z
C	-4.207	-2.253	-0.186
C	-3.472	-1.084	-0.301
C	-2.047	-1.101	-0.176
C	-1.419	-2.360	0.047
C	-2.172	-3.519	0.154
C	-3.568	-3.478	0.043
H	-5.290	-2.216	-0.280
H	-3.968	-0.137	-0.494
H	-0.338	-2.397	0.135
H	-1.671	-4.468	0.328
H	-4.150	-4.391	0.128
C	-1.321	0.084	-0.306
C	-1.464	1.468	-0.155
C	-0.757	2.385	-0.982
C	-2.308	2.004	0.863
C	-0.898	3.753	-0.806
H	-0.103	1.993	-1.755
C	-2.444	3.375	1.019
H	-2.839	1.318	1.517
C	-1.742	4.259	0.190
H	-0.351	4.436	-1.450
H	-3.095	3.764	1.798
H	-1.849	5.332	0.322
C	3.628	-0.476	0.102
F	4.109	0.107	1.207
F	4.240	0.055	-0.965
F	3.908	-1.786	0.150
Br	1.671	-0.199	-0.023
E=-3414.1927609, ZPE=0.1932888			

Table S20. Cartesian coordinates of **12b** calculated at the B97D3/def2-TZVP level of theory.			
Atomic Symbol	x	y	z
C	1.715	2.817	0.258
C	0.644	1.935	0.274
C	0.564	0.860	-0.653
C	1.631	0.718	-1.577
C	2.696	1.608	-1.584
C	2.748	2.667	-0.672
H	1.756	3.618	0.992
H	-0.125	2.039	1.031
H	1.604	-0.096	-2.293
H	3.494	1.478	-2.311
H	3.587	3.357	-0.678
C	-0.554	-0.044	-0.604
C	-1.864	0.257	-0.079
C	-2.686	-0.722	0.529
C	-2.383	1.573	-0.185
C	-3.940	-0.394	1.029
H	-2.318	-1.738	0.620
C	-3.640	1.890	0.311
H	-1.797	2.332	-0.693
C	-4.427	0.912	0.927
H	-4.543	-1.163	1.504
H	-4.018	2.903	0.201
H	-5.411	1.163	1.314
C	2.133	-0.906	1.477
F	2.726	-2.025	1.065
F	1.148	-1.174	2.336
F	3.018	-0.067	2.014
Br	-0.288	-1.815	-1.290
E=-3414.250842, ZPE=0.1945568			

Table S21. Cartesian coordinates of **13b** calculated at the B97D3/def2-TZVP level of theory.			
Atomic Symbol	x	y	z
C	-2.627	2.023	-1.253
C	-1.467	1.275	-1.092
C	-1.306	0.415	0.007
C	-2.343	0.325	0.942
C	-3.506	1.082	0.782
C	-3.655	1.931	-0.311
H	-2.729	2.678	-2.114
H	-0.672	1.348	-1.828
H	-2.262	-0.322	1.805
H	-4.297	1.001	1.523
H	-4.564	2.515	-0.432
C	0.004	-0.348	0.102
C	1.224	0.565	-0.013
C	2.429	0.156	-0.592
C	1.152	1.842	0.564
C	3.532	1.008	-0.610
H	2.501	-0.828	-1.042
C	2.258	2.690	0.552
H	0.229	2.173	1.027
C	3.452	2.278	-0.039
H	4.457	0.674	-1.074
H	2.181	3.675	1.003
H	4.312	2.942	-0.057
C	0.163	-1.224	1.381
F	0.143	-0.432	2.486
F	-0.815	-2.144	1.531
F	1.338	-1.885	1.392
Br	-0.029	-1.709	-1.429
E=-3414.3444342, ZPE=0.199022			

Table S22. Relative energies of **T-6**, **S-6**, **T-10a** and **S-10a** at different levels of theory. All energies in kcal/mol.

	T-6	**S-6**	**T-10a**	**S-10a**
B97-D3/def2-TZVP	0.0	6.1	-6.1	-10
B97-D3/def2-TZVP//CHARMM	0.0	5.3	-	-
CAS(8,8)MP2/6-31G*	0.0	9.2	-	-
BLYP-D3/def2-TZVP	0.0	3.3	-5.9	-13.4
B3LYP-D3/def2-TZVP	0.0	5.7	-5.0	-8.8
B3LYP-D3/6-311G**	0.0	5.7	-5.4	-9.0
B3LYP/6-311G**	0.0	6.3	-1.1	-3.9
M06-2X/def2-TZVP	0.0	6.8	-4.3	-3.9
wB97X/def2-TZVP	0.0	8.7	-4.0	-1.8
wB97XD/def2-TZVP	0.0	7.6	-4.3	-3.7

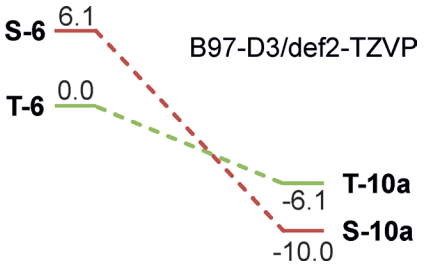

References

1. Gaussian 09, Revision D.01, Frisch, M. J.; Trucks, G. W.; Schlegel, H. B.; Scuseria, G. E.; Robb, M. A.; Cheeseman, J. R.; Scalmani, G.; Barone, V.; Mennucci, B.; Petersson, G. A.; Nakatsuji, H.; Caricato, M.; Li, X.; Hratchian, H. P.; Izmaylov, A. F.; Bloino, J.; Zheng, G.; Sonnenberg, J. L.; Hada, M.; Ehara, M.; Toyota, K.; Fukuda, R.; Hasegawa, J.; Ishida, M.; Nakajima, T.; Honda, Y.; Kitao, O.; Nakai, H.; Vreven, T.; Montgomery, J. A., Jr.; Peralta, J. E.; Ogliaro, F.; Bearpark, M.; Heyd, J. J.; Brothers, E.; Kudin, K. N.; Staroverov, V. N.; Kobayashi, R.; Normand, J.; Raghavachari, K.; Rendell, A.; Burant, J. C.; Iyengar, S. S.; Tomasi, J.; Cossi, M.; Rega, N.; Millam, J. M.; Klene, M.; Knox, J. E.; Cross, J. B.; Bakken, V.; Adamo, C.; Jaramillo, J.; Gomperts, R.; Stratmann, R. E.; Yazyev, O.; Austin, A. J.; Cammi, R.; Pomelli, C.; Ochterski, J. W.; Martin, R. L.; Morokuma, K.; Zakrzewski, V. G.; Voth, G. A.; Salvador, P.; Dannenberg, J. J.; Dapprich, S.; Daniels, A. D.; Farkas, Ö.; Foresman, J. B.; Ortiz, J. V.; Cioslowski, J.; Fox, D. J. *Gaussian, Inc., Wallingford CT* **2009**.

2. Yamamoto, N.; Vreven, T.; Robb, M. A.; Frisch, M. J.; Schlegel, H. B. *Chem. Phys. Lett.* **1996**, *250*, 373-378.

3. Hay, P. J.; Wadt, W. R. *J. Chem. Phys.* **1985**, *82*, 299-310.

4. Head-Gordon, M.; Pople, J. A.; Frisch, M. J. *Chem. Phys. Lett.***1988**, *153*, 503-506.

5. McDouall, J. J.; Peasley, K.; Robb, M. A. *Chem. Phys. Lett.* **1988**, *148*, 183-189.

6. Abegg, P. W.; Ha, T. K. *Mol. Phys.* **1974**, 27, 763-67.